Geomechanics and Engineering, *Vol. 42, No. 3 (2025) 229-241*
https://doi.org/10.12989/gae.2025.42.3.229

Underground space reservation and surface subsidence prediction based on key pillar mining and backfilling

Jinhai Zhao[1,2a], Congcong Niu[1,2b], Liming Yin*[1,2], Weilong Zhu[1,2c] and Xinguo Zhang[1,2d]

[1]*College of Energy and Mining Engineering, Shandong University of Science and Technology, Qingdao 266590, China*
[2]*State Key Laboratory Breeding Base for Mining Disaster Prevention and Control, Shandong University of Science and Technology, Qingdao 266590, China*

(*Received April 27, 2024, Revised July 21, 2025, Accepted July 22, 2025*)

Abstract. As the core technical scheme to protect the surface buildings (structures) in the mining area, the short-wall continuous mining and filling technology plays an irreplaceable role in the field of mining. The jump mining distance and the control characteristics of overlying strata are the key factors affecting the construction scope of underground space and the stability of overlying strata, which directly determine the safety and reliability of mining engineering. Different skip mining modes will form different underground space structures, and the scientific and reasonable comprehensive development and utilization of these underground spaces is an important breakthrough to fully tap the added value of filling mining and improve the comprehensive benefits of resources. In order to effectively control the stability of overlying strata in goaf, based on the short-wall paste continuous mining and filling technology, this study proposes a collaborative optimization method of continuous mining and filling and key pillar filling. On the basis of traditional filling technology, the space utilization rate and economic benefits of goaf are further improved. In this paper, three kinds of skip-mining modes and corresponding bearing structures are designed, which are named as Common Single Stripe Elements Backfilling while Mining (CSEBM), Trinity Stripe Elements Backfilling while Mining (TRSEBM) and Twosome Stripe Elements Backfilling while Mining (TWSEBM), respectively. The corresponding supporting technology and parameters are optimized, and the stress distribution characteristics under different filling skip-mining modes are revealed by COMSOL numerical simulation. Based on the geological conditions of a mining area in Shanxi Province, this paper uses the probability integral method to predict the surface subsidence law after mining, and obtains the surface subsidence, horizontal movement, horizontal deformation and curvature distribution characteristics under different skip filling methods. The comparative analysis shows that the surface settlement, horizontal displacement, deformation and curvature of the scattered pillar filling scheme are the smallest, and the damage area of the filling column itself is small, which can significantly improve the volume efficiency of space construction, and lay a solid foundation for the deep development and diversified space utilization of underground space resources.

Keywords: backfilling mining; continuous mining and continuous backfilling; key pillar backfilling; simulation; underground space reservation

1. Introduction

With the exploitation of coal resources, the problems of goaf collapse and soil erosion are becoming more and more serious. The treatment of goaf has become an urgent problem to be solved. Backfilling mining technology is one of the effective ways to solve the problems of goaf collapse and environment. Backfilling mining is to decompose the solid waste and garbage produced in the process of coal mining and then fill it into the goaf, which can effectively reduce the subsidence space of the roof strata, so as to achieve the purpose of controlling the movement of the strata and reducing the surface subsidence. It is a green mining method. The technology of early coal Backfilling mining mainly includes hydraulic backfilling (Wang and Zhang 2009) wind backfilling (Hua *et al*. 1995) and water sand backfilling (Ugurlu and Ozturk 2021, Wu and Li 2011). Subsequently, significant advancements have been made in backfilling technology along with improvements in mining practices.At present, the backfilling mining methods are mainly divided into solid backfilling (Hu *et al.* 2020, Liu *et al.* 2020a, Yang *et al.* 2013, Miao *et al*. 2010), paste backfilling (Wang *et al*. 2019, Huang *et al*. 2021), high water backfilling (Yang 2023, Wu *et al.* 2023, Sun 2022, Bai *et al.* 2022, Li *et al*. 2020), ultra-high water backfilling (Rajeev *et al.* 2016, Khaldoun *et al*. 2016, Widisinghe and Sivakugan 2014, Yu *et al*. 2020, Meng *et al*. 2023) and other types according to the characteristics of backfilling materials. Among them, paste backfilling has the best control effect on the surface, and the backfilling cost is

*Corresponding author, Master
E-mail: yinliming@sdust.edu.cn
[a]Professor
E-mail: Jinhai.zhao@sdust.edu.cn
[b]Master
E-mail: n18364048867@163.com
[c]Master
E-mail: zwl0315224@163.com
[d]Professor
E-mail: skd992993@sdust.edu.cn

ISSN: 2005-307X (Print), 2092-6219 (Online)

relatively low. It is widely used in underground production disaster prevention and surface subsidence control in major mining areas. The paste backfilling can be divided into two backfilling methods: long-wall fully mechanized paste post-frame backfilling and short-wall paste continuous mining and continuous backfilling. Among them, the long-wall fully mechanized paste post-frame backfilling process system is complex and the cost is high. The short-wall paste continuous mining and continuous backfilling method has the characteristics of simple system, low investment and low cost. With the rapid development and use in China, it has become one of the mainstream backfilling mining methods.As the current mainstream coal mining technology, paste backfilling mining has great which are embodied in the following aspects: (1) High backfilling rate, high strength after solidification, and good effect of reducing surface subsidence. (2) The high utilization rate of materials is conducive to the protection of the environment. (3) It can liberate more coal resources and improve the rate of coal output. (4) The backfilling material and the surrounding rock form a good system, which reduces the occurrence of rock burst and ensures the safety.

Paste backfilling involves crushing coal gangue and other solid waste, mixing them with fly ash, and adding water to form a paste slurry (Sun 2021, Wang *et al*. 2019, Lu *et al*. 2023, Wang *et al.* 2020). Through pipeline transportation, it is filled into the goaf with a backfilling pump, and the overlying strata can be supported after solidification to reduce surface subsidence. The main process flow : backfilling preparation → pipe backfilling → mortar pushing water → gangue pushing mortar → mortar pushing gangue → water pushing mortar → pipe cleaning → blowing. Paste backfilling has the advantages of good slurry fluidity, high density and high strength of backfilling body, which can effectively control rock movement and surface subsidence. Paste backfilling technology has nearly 30 years of development history in metal mines. The earliest application in coal mines is Germany. In 2004, China 's coal mines began to carry out experimental research and application of paste backfilling coal mining in Fengfeng, Jiaozuo, Zibo and other mining areas (Xu 2021). Yang (2023) studied the law of surface subsidence and overburden movement and failure caused by paste backfilling mining, and concluded that the backfilling rate of paste backfilling had a great influence on the failure of overburden movement and was less affected by strip width and backfilling strength. Wang studied the effect of different water content on the uniaxial compressive mechanical behavior of paste backfilling materialsm (Wang *et al.* 2022). It was found that the higher the water content, the lower the uniaxial compressive strength of paste backfilling specimens and the decrease rate gradually accelerated with the increase of water content.

The key pillars refer to the remaining coal pillars in the goaf that are likely to experience local instability first. The slightly more stable remaining coal pillars in the adjacent area of the key pillars are called “sub-key pillars.” Feng Guorui proposed a method for distinguishing key pillars. Bai Jinwen proposed the key column side backfilling technology for the key column in view of the chain instability of the remaining coal pillar group, which not only can be effectively used for the prevention and control of the chain instability of the remaining coal pillar group in the goaf, but also can be applied to the technical fields such as the re-mining of high-quality remaining coal resources and the maintenance and utilization of underground space (Bai *et al*. 2021, Feng *et al.* 2023). Cui Boqiang studied the mechanical properties, failure and instability characteristics of the coal-filled structure with unilateral backfilling beside the column, and found that the volume ratio of coal components has an important influence on the mechanical properties of the coal-filled structure (Cui *et al*. 2023). The larger the volume ratio of coal components, the more likely it is to cause sudden instability of the structure.

To further enhance the construction efficiency of underground spaces and innovate the integration of coal mining with backfilling techniques, this study proposes a synchronized approach to orderly construction and efficient backfilling of mined-out areas during mining operations. This technical pathway not only ensures safe and efficient coal resource extraction but also effectively extends industrial chains through rational development and utilization of underground spaces, significantly increasing the comprehensive added value and resource utilization efficiency of coal mining. Based on the shortwall paste continuous mining and backfilling process, this paper proposes three skip mining backfilling methods for constructing underground spaces: continuous backfilling of unit columns, centralized central pillar backfilling, and decentralized central pillar backfilling, along with corresponding support techniques and parameters. Numerical simulations analyzed the three key column backfilling methods, obtaining characteristics such as stability, economic efficiency, and load-bearing capacity of backfill columns. Using the probabilistic integral method, surface subsidence caused by mining was predicted, generating maps of surface subsidence, curvature, horizontal displacement, and horizontal deformation. The study evaluated the surface control effects of the three key column backfilling methods. These research findings provide significant reference value for enriching backfill mining theories, supporting mined-out area backfilling and utilization, while enhancing local available space that promotes secondary development of mined-out areas. This lays the foundation for future research on pumped storage power generation and carbon dioxide storage utilization models.

2. Introduction to short wall continuous mining and filling mining technology

2.1 Design of short wall continuous mining and continuous backfilling working face

The layout of the working face is similar to that of the long wall working face. The lower crossheading is used for air intake and transportation, the upper crossheading is used for air return and backfilling, and the branch roadway is ventilated by local fan. The layout of the working face is arranged in the way

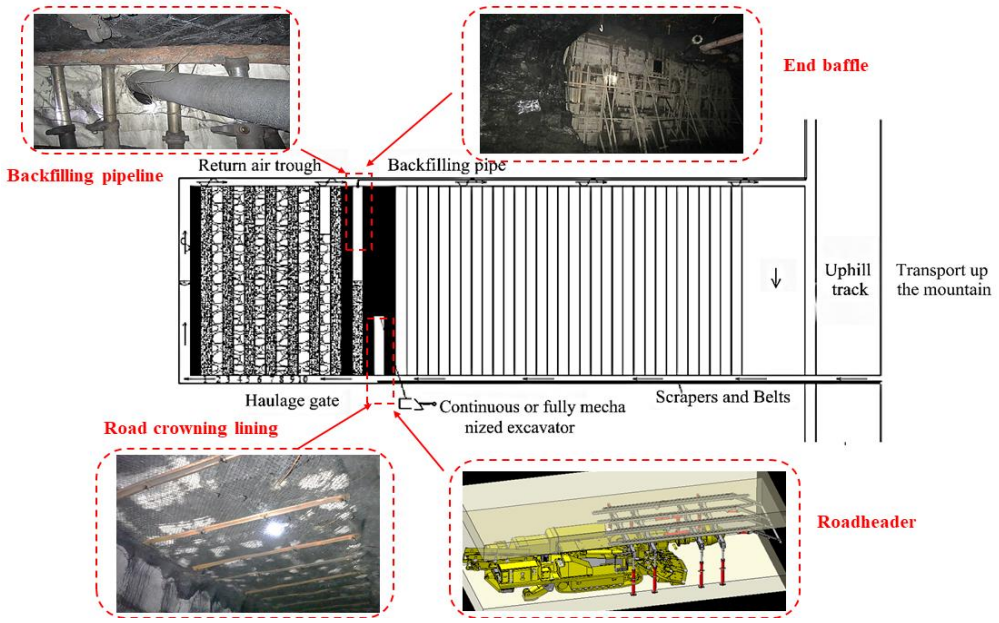

Fig. 1 Short arm continuous mining and continuous backfilling working face mining backfilling production cycle diagram

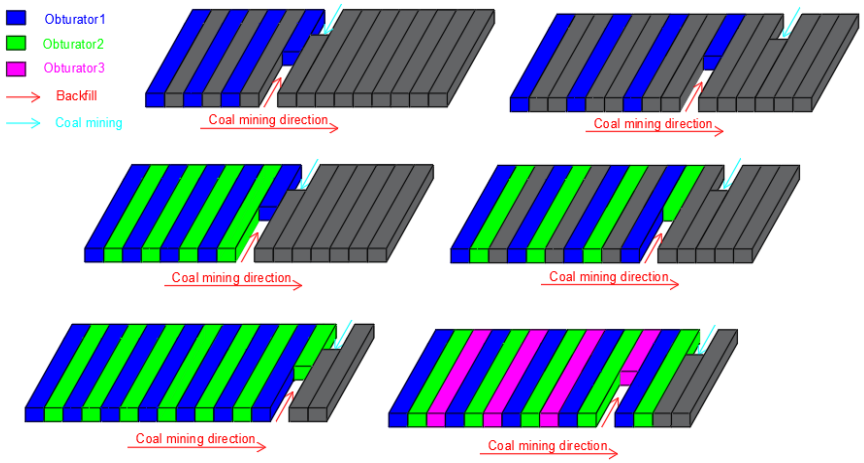

Fig. 2 Two backfilling mining modes

of double entry and one return and three entry and one return. The design of the working face is determined by the supporting equipment. The mining and backfilling production cycle of the short-wall continuous mining and continuous backfilling working face is shown in Fig. 1.

There are two main backfilling mining modes, namely, one mining every other and one mining every other, and two-step and three-step modes are realized respectively, as shown in Fig. 2. BackFilling is carried out immediately after the completion of each branch roadway mining, and the next branch roadway is mined at the same time; Backfilling and coal mining do not interfere with each other, continuous parallel operation, mining and backfilling the remaining branch roadway in turn. According to the relevant specifications and requirements, the protective coal pillars set in the working face are recovered to realize the full mining and full backfilling of the working face. For thick coal seams, the branch roadway adopts layered mining and the whole roadway is backfilled.

The thick coal seam is divided into upper layer and lower layer, two continuous shearers, two loaders and one bolt trolley work at the same time; the No.1 continuous miner specializes in mining the upper layer, and the No.2 continuous miner specializes in mining the lower layer. Two continuous mining machines work continuously in two roadways, and the bolt trolley is alternately supported. At the same time, the whole branch roadway of the upper and lower layers has been backfilled. Filling and coal mining do not interfere with each other, realize continuous mining and continuous backfilling of the working face, solve the contradiction between mining and backfilling, maximize the parallel operation of mining and backfilling, and improve the efficiency of backfilling coal mining (Li *et al.* 2021).

The utilization of continuous mining and continuous backfilling technology not only enhances the availability and economy of goaf over traditional backfilling methods, but also increases the effective volume of each local goaf, thereby

Table 1 Comparison of three filling schemes

Filling scheme	merit	defect
CSEBM	1. The single mining and filling length is short (both b), with high construction flexibility. 2. The frequent alternation of mining and filling enables rapid support of the goaf, resulting in good short-term stability.	1.The number of mining and filling cycles is large, resulting in poor process continuity and increased construction time and costs. 2.The filling columns are densely distributed, leading to poor overall coordination.
TRSEBM	1.The single mining and filling length is long (both 3b), with fewer mining and filling cycles and high early-stage benefits. 2.The centralized arrangement of filling columns can form a stronger backbone support structure, featuring strong long-term bearing capacity.	1.The goaf exposure time is longer, which requires higher support strength. 2.The filling time is longer, leading to higher support time, greater costs, and a wider scope.
TWSEBM	1.The single mining and filling length (both 2b) falls between the previous two, balancing construction efficiency and early-stage costs. 2.The stress distribution of filling columns is more uniform, with better overall coordination.	1.The number of mining and filling cycles is greater than that of centralized pillar filling, and the process continuity is inferior to the latter. 2.Compared with ordinary column filling, the single operation range is larger, making short-term stability control slightly more difficult.

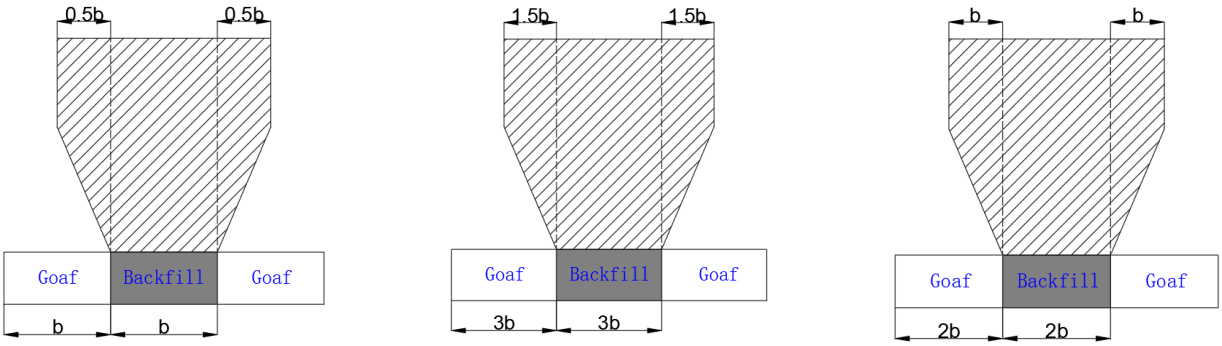

(a) (b) (c)

Fig. 3 Mechanical diagram of three backfilling schemes

laying the groundwork for further exploration of goaf applications, such as pumped storage power generation and carbon dioxide storage.

This paper proposes three column-backfilling mining methods based on the short-wall paste continuous mining and continuous backfilling process.

The first method is CSEBM, whereby the size of the backfilling column is consistent with the size of the goaf. It involves mining a coal interval by backfilling one column and then backfilling another column. The second method is TRSEBM, where the size of the backfilling column is three times larger than that of CSEBM. This method expands the space of the goaf. The third method is TWSEBM, where two pillars are filled to mine two coal intervals Fig. 3 shows the mechanical schematic diagram of the three backfilling schemes: (a) CSEBM, (b) TRSEBM, and (c) TWSEBM.

Each of the three filling schemes has its advantages and disadvantages: CSEBM offers high short-term stability but is low in efficiency and high in cost; TRSEBM boasts high filling efficiency and strong long-term bearing capacity, yet requires high support strength and incurs significant costs; TWSEBM balances efficiency and cost, but falls short of the first two in terms of short-term efficiency and stability. All three have certain limitations: ordinary column filling may affect the construction period due to its inefficiency; centralized filling could increase safety risks owing to its high support requirements; and dispersed filling demands precise control to address issues such as efficiency.

2.2 Determination of the width of branch roadway

In the short-wall paste backfilling interval skip mining technology, the roof of the mining space can be considered as a “beam” structure supported by coal pillars on both sides. Due to the limited mining range, the coal pillar effectively holds the roof in place. Therefore, the stability of the rock beam is calculated as a “simply supported beam,” as depicted in Fig. 4.

The maximum normal stress σmax and maximum shear stress τxy in the beam are:

Where: H-beam height (m);

L-beam width (m).

In the extreme case, the maximum span of the rock beam, taking into account the impact of the highest tensile stress in the rock beam, should be

$$L = \sqrt{\frac{4h^2 R_t}{3qF_0}} \tag{1}$$

The ultimate span of rock beam considering the influence

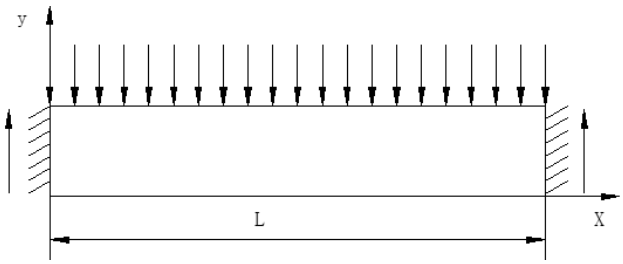

Fig. 4 Roof simply supported beam structure model

of maximum shear stress in rock beam

$$L = \frac{4hR_j}{3qF_0} \tag{2}$$

In the formula: F0-safety factor, take 2-4; Rt-tensile strength; Rj - shear strength. Among them, the load q is the load of the roof rock beam.

$$\mathrm{q} = \frac{\mathrm{E_1 h_1}^3 \left(\sum \rho_n h_n \right)}{\sum E_n {h_n}^3} \tag{3}$$

The collapse of the immediate roof is crucial in determining the layout of the mining unit on the working face when employing backfilling mining technology.The initial caving step of the immediate roof is calculated based on the thickness histogram of the rock strata and the lithology of each rock stratum (including bulk density, elastic modulus, uniaxial compressive strength, and other indicators) in the working face. Additionally, comprehensive determination of the width of a mining unit is carried out by considering the construction factors of the coal mining site and the coal cutting range of the roadheader.

2.3 Length design of working face

The length of the short-wall paste backfilling interval skip mining face is determined based on the following factors:

(1) Minimize the number of roadheader turns and maximize the length of the branch lane. If the branch roadway is too short, it results in excessive roadheader movements, negatively impacting production and efficiency.

(2) It is crucial to ensure that the rear continuous transportation system of the roadheader has an adequate length to enhance tunneling efficiency.

(3) The length of the branch roadway directly influences the cost per ton of coal, encompassing tunneling, maintenance, and transportation costs. Generally, for coal seams with dip angles ranging from 8 to 12 degrees, a length of 100-160 m is considered appropriate when calculating the length of the branch roadway.

2.4 Roadway support design

When the short-wall continuous mining and continuous backfilling excavation roadway is excavated, the excavation roadway is supported, and the borehole is drilled and the bolt is installed in the space where the rock layer is mined. According to the initial support strength and the specific geological rock properties, the size of the mine pressure to determine the drilling and anchor installation density.

The bolt parameters are designed according to the suspension theory, and the calculation method is as follows:

(1) Anchor length

$$L = L_1 + L_2 + L_3 \tag{4}$$

In the above formula, L:the length of the anchor; L1: the exposed length of the anchor, m; L_2: effective length of bolt, m; L_3:Anchor bolt is anchored into the stable coal wall, and the value is 0.3 m.

① The determination of the exposed length L1 of the anchor rod

L1 = iron plate thickness + nut thickness + (0.02-0.03) m, take L1 = 0.1 m.

② Determination of the effective length L2 of the bolt

$$L_2 = 1 / f \times [B / 2 + H \times tan(45^0 - w / 2)] \tag{5}$$

H-roadway excavation height in-type ; ω side-internal friction angle of surrounding rock of two sides ; f-Prussian coefficient ; b-roadway excavation width ;

(2) Determination of row spacing between bolts

According to the support experience of the adjacent working face of the mine, the row spacing between the bolts can be calculated according to the empirical formula

$$d \le 0.6L \tag{6}$$

In the formula, d-bolt spacing, row spacing, m.

(3) Determination of bolt diameter

$$d = \sqrt{\frac{4Q}{\pi\sigma}} \tag{7}$$

The length of d-anchor in formula

Q-anchor design anchorage force;

σ-anchor tensile strength

Due to the large spatial span of the goaf with concentrated central pillar, the calculation method of anchor cable support with anchor cable support is as follows:

(1) Anchor cable length

According to the design principle of anchor cable strengthening support, the length of anchor cable depends on the lithology of roadway roof, rock mass structure, roadway engineering size and stable rock stratum position. The anchorage section of the anchor cable requires that the anchorage into the stable rock layer is not less than 2 m.

$$L_s = L_{s_1} + L_{s_2} + L_{s_3} \tag{8}$$

In the formula, the length of Ls-anchor cable, m ; L_{s1}-

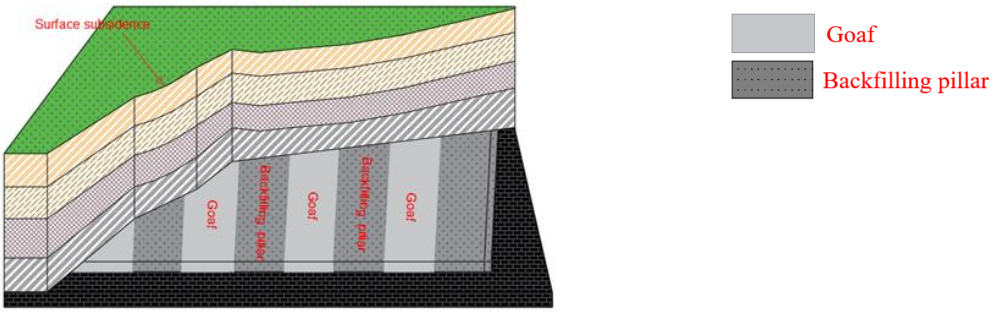

(a) CSEBM empty area support

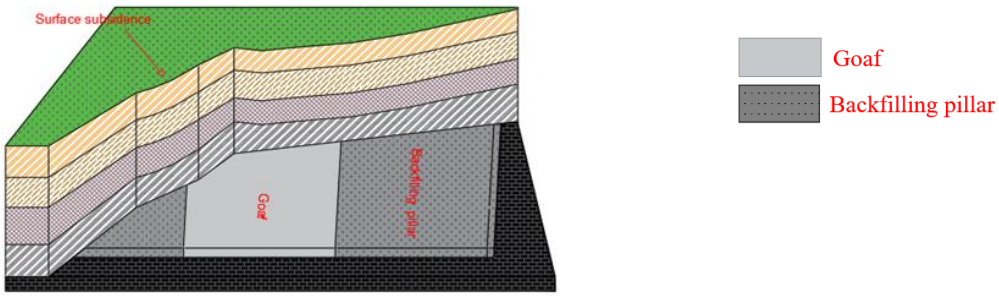

(b) TRSEBM empty area support

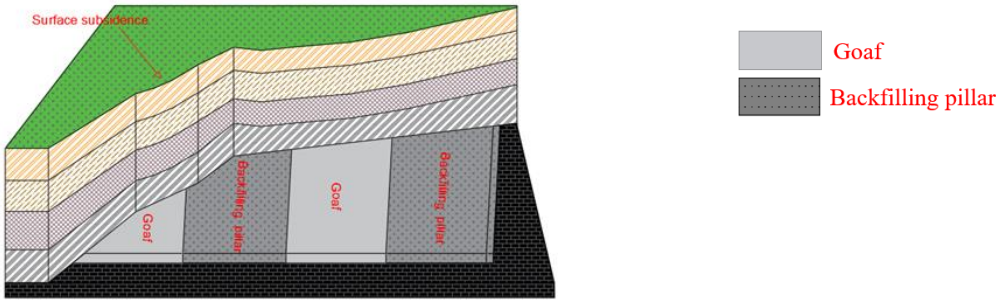

(c) TWSEBM empty area support

Fig. 5 Three kinds of key pillar backfilling empty area support diagram

The length of the exposed roof of the anchor cable, L_{s2}-The height of the potentially unstable rock strata, L_{s3}-The anchor cable is anchored into the stable rock strata not less than 2 m.

(2) Diameter of anchor cable borehole

According to the matching requirements of " three diameters, " the difference between the diameter of the anchor hole and the diameter of the anchor rod is 6~10 mm, and the difference between the diameter of the anchor hole and the diameter of the resin anchoring agent is 4~8 mm.

(3) Determination of row spacing between anchor cables

The row spacing of anchor cable is calculated according to the following formula

$$a_s = 0.887d\sqrt{\frac{\sigma_t}{k\gamma l_2}} \tag{9}$$

α_s-Anchor cable spacing, row spacing;d-Anchor cable diameter;σ_t-Tensile strength of anchor cable;k-Factor of safety, Generally take 1.5~1.8; l_2-Roadway roof fracture zone height; γ-The average gravity density of the rock layer is anchored by the anchor cable, and the sandstone density value is taken.

After the initial support is completed, the unexploited strip rock pillar in the first step is mined again, and the second borehole is drilled and the second bolt is installed in the space where the strip rock pillar is mined to support the roadway. The installation density of the second borehole and the second bolt is determined according to the initial support strength, the specific geological rock properties and the size of the mine pressure.

3. Numerical simulation analysis of three backfilling methods

3.1 Numerical simulation analysis

In this paper, three backfilling methods are proposed, which are CSEBM, TRSEBM and TWSEBM. After coal mining, the underground goaf is left behind, causing surface subsidence and instability, which is easy to cause collapse. Coal backfilling column can effectively prevent the settlement of the surface in the process of coal mining, and play a supporting role on the surface. In this paper, the finite element mechanics analysis software COMSOL Multiphysics is used

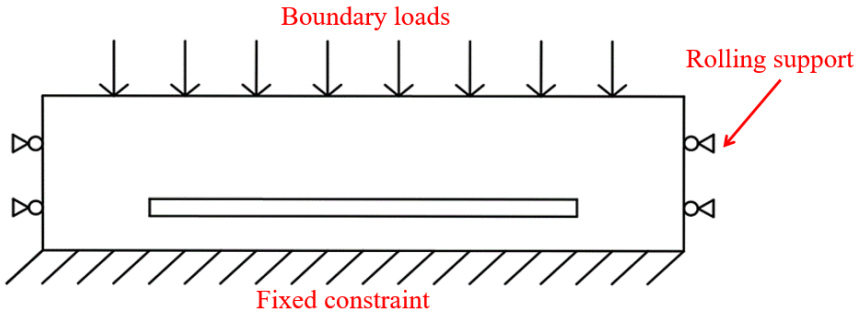

Fig. 6 Geometric model

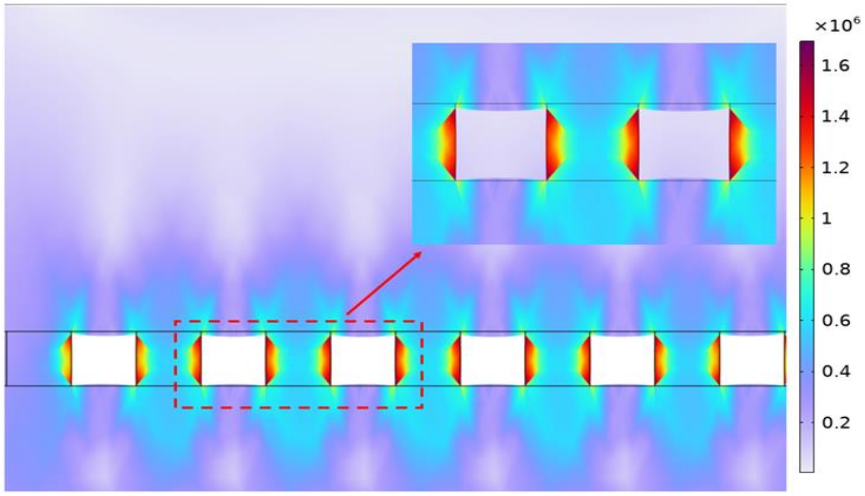

Fig. 7 Vertical stress diagram of CSEBM before and after excavation

for numerical simulation. The numerical simulation method is now widely used in geotechnical mechanics. It is used to solve the stability problems of surrounding rock stress, mining site pressure and analysis of tunnel, excavation, slope stability and retaining structure. It is an effective numerical simulation analysis method to accurate ely predict the mechanical properties of rock mass and solve complex geotechnical problems. The software is used to realize the numerical simulation of CSEBM, TRSEBM and TWSEBM in mining area, and the stress distribution is obtained.

3.2 Construction of the model

(1) The geometric size of the two-dimensional numerical model: The geometric size of the model is 180 m × 45 m, the excavation section is rectangular, and the size of the excavation rectangle is discussed in three cases. In the first CSEBM scheme, the excavation size of rectangular roadway is 10 m × 5 m, and the backfilling size of key column is 10 m × 5 m. In the second TRSEBM scheme, the excavation size of the rectangular roadway is 30 m × 5 m, and the size of the middle column is 30 m × 5 m. In the third TWSEBM scheme, the excavation size of the rectangular roadway is 20 m × 5 m, and the backfilling size of the middle column is 20 m × 5 m (Fig. 6).

(2) Boundary conditions : The left and right sides of the model are roller supports, which are used to restrict the motion of the object. The displacement of the object in the normal direction is restricted, so that it can only move in the tangential direction. A fixed constraint is applied at the bottom to limit the movement of the lower surface of the model.;that is, the displacements are zero in all directions on the selected geometrical entities. If there are rotational degrees of freedom, they will also be zero.The entire geometric model adds a gravity domain to simulate gravity.

(3) Material parameters are shown in Table 2.

Table 2 Parameter indexes of geometric model materials

poisson ratio (μ)	Density (ρ/[kg/m³])	Young's modulus (E/MPa)
0.4	2000	20

Poisson's ratio: an elastic constant that reflects lateral deformation of a material.
Yang's modulus: describes the ability of a solid material to resist deformation.

3.3 Analysis of the stress characteristics of the paste backfilling column of the three schemes

3.3.1 Analysis of the stress characteristics of the backfilling column of the ordinary backfilling scheme

Fig. 7 is the vertical stress diagram obtained after CSEBM excavation. From the diagram, it can be seen that the minimum stress value of the backfilling column is 0.6

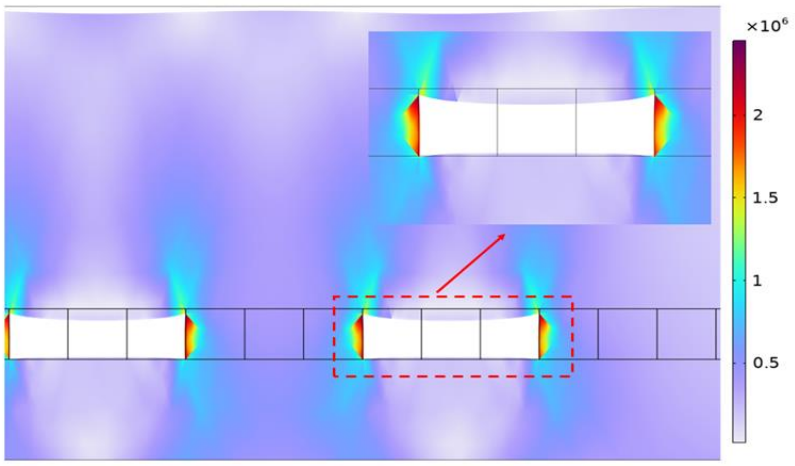

Fig. 8 Vertical stress diagram of TRSEBM after excavation

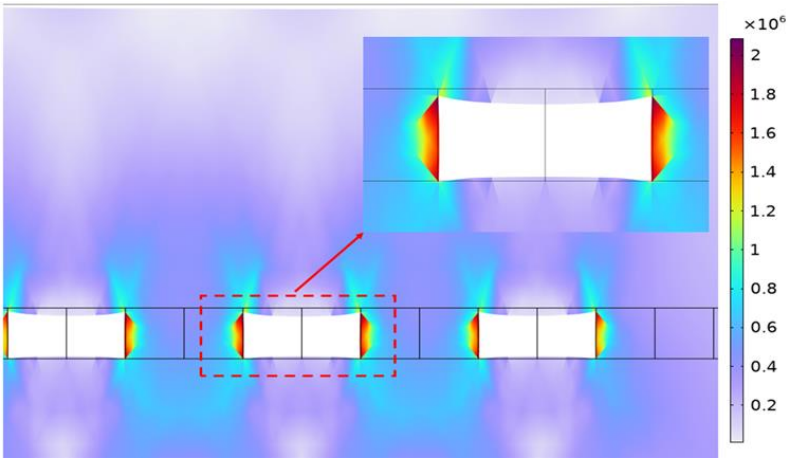

Fig. 9 Vertical stress diagram of TWSEBM after excavation

Mpa, and the maximum value is 1.6 Mpa. The stress in the middle of the backfilling column is the smallest. The stress on both sides of the column wall is the largest, which gradually increases from the middle to the surrounding, and the stress on the side of the two columns presents a T-shaped shape.

3.3.2 Analysis of the stress characteristics of the centralized pillar backfilling scheme

The vertical stress diagram of the TRSEBM scheme after excavation is shown in Fig. 8.The stress in the middle of the backfilling column is relatively uniform, and the stress values on both sides are abrupt. The stress value in the column is about 0.5 Mpa, and the maximum stress on both sides is about 2.5 Mpa. The internal stress of the whole goaf presents a concave rectangle, and the stress in the upper part is smaller than that in the wall side, and the stress change range is larger.

3.3.3 Analysis of stress characteristics of scattered small and medium pillar backfilling scheme

Fig. 9 is the vertical stress diagram of TWSEBM after excavation. It can be seen from the figure that when the goaf is excavated, the stress value of the middle part of the small backfilling column reaches 0.6 Mpa, and the maximum stress on both sides reaches 2 Mpa. After excavation, the stress value around the backfilling column shows an outward radiation-like shape, and the surrounding stress value is 0.6 Mpa. The farther the distance between the inner stress of the column wall and the central axis is, the greater the stress is.

3.4 Cost and space analysis of three backfilling schemes

In the above three backfilling column mining schemes, the area of the backfilling column is the same as the backfilling column material. The maximum size of the space left by the CSEBM scheme is 10 m × 10 m, the space left by the TRSEBM scheme can reach 30 m × 10 m, and the space left by the TWSEBM scheme is 20 m × 20 m.

From the vertical stress diagram after excavation, it can be seen that the maximum vertical stress value at the two sides of the backfilling column after CSEBM scheme mining is 1.6 Mpa, the maximum vertical stress value after TRSEBM scheme excavation is 2.5 Mpa, and the maximum stress value in the column after TWSEBM backfilling scheme mining is 2 Mpa. The backfilling strength of 6% cement grouting can

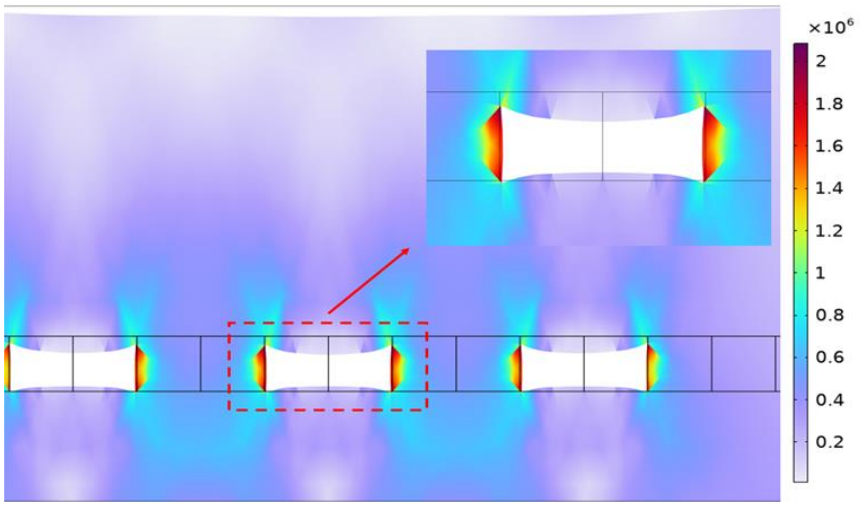

Fig. 10 TWSEBM reduces the vertical stress diagram of elastic modulus

reach 4 Mpa, the cost of CSEBM is the lowest, the cost of TWSEBM is lower, and the cost of TRSEBM is the highest. The goaf space left by CSEBM is small. Although the TRSEBM scheme has a large space, the high cost requires a large strength of the backfilling column, while the goaf space left by the TWSEBM scheme is large. Therefore, considering the cost and the size of the goaf, the TWSEBM scheme has the best cost and space.

For the third optimal TWSEBM scheme, the elastic modulus is doubled, and the vertical stress under this condition is studied. The results show that the maximum stress value is 2MPa, which is located on the side of the backfilling column wall on one side of the goaf. The vertical stress in the upper part of the goaf develops downward, and the vertical stress in the lower part develops upward. The vertical stress is shown in Fig. 10. Therefore, the vertical stress obtained by the TWSEBM scheme is still good under the condition of reducing the elastic modulus by half.

Therefore, the TWSEBM scheme improves the available space and economy of the goaf, and lays a certain foundation for the research on the utilization methods of coal mine underground reservoir, pumped storage power generation and carbon dioxide storage in the western ecologically fragile area.

4. Strength design of backfilling column

The backfilling material selection of the backfilling column has an important influence on the strength of the column, cost control and later maintenance. The backfilling material of the column can select the coal gangue, fly ash and cement left in the mining area during the coal mining process as the backfilling material.

From the above diagram, it is known that the maximum vertical stress value of CSEBM after excavation in the three schemes is 1.6 Mpa, the maximum stress of the column after excavation in the TRSEBM scheme is 2.5 Mpa, and the maximum vertical stress value of the backfilling column after excavation in the TWSEBM scheme is 2Mpa.Therefore, at least the strength value of the backfilling material can reach 2.5 Mpa to ensure the strength safety of the column. According to the previous research results(Chang *et al.* 2022), the ratio of backfilling material coal gangue, fly ash, gypsum, cement and mine water is 74: 2: 2: 7: 15, and the slurry concentration is 85%. The compressive strength of the backfilling body is 2.93 MPa, 3.01 MPa and 3.10 MPa at the age of 9,15 and 28 d, respectively. It can be seen that under the above ratio, the uniaxial compressive strength of the backfilling body can reach 3.0 MPa after the age of the backfilling body reaches 28 d, which meets the strength requirements of the backfilling column.

The backfilling body is in a unidirectional stress state after paste backfilling mining. Theoretically, there are four formulas for calculating the allowable strength [σ] of coal body under uniaxial stress state, which are Obert-Kwvall/Wang formula, Holland formula, Salamon-Mnuro formula and Bieniawski formula. Because the paste backfilling material is a dense whole, there are few joint cracks, and the overall performance is good. The stress deformation and failure are typical plastic and brittle failure characteristics. The overall paste shows good plastic characteristics, and with the change of time and roof pressure, the strength is further increased. The late strength requirement of comprehensive paste backfilling is calculated according to Bieniawski. According to the Bieniawski formula, the allowable strength of the backfilling body can be calculated by the following formula

$$[\sigma] = \sigma_m \left(0 \cdot 64 + 0 \cdot 36 \frac{w}{h}\right)^n \tag{10}$$

where: W / h - Width-Height ratio of coal pillar; when w / h > 5, take 1.4, otherwise take 1.

CSEBM: $[\sigma] = \sigma_m \left(0 \cdot 64 + 0 \cdot 36 \frac{w}{n}\right)^n = \sigma_m (0.64 + 0.36 \frac{5}{3.5})^1$ =3MPa,factor of safety is 2.6.

TRSEBM: $[\sigma] = \sigma_m \left(0 \cdot 64 + 0 \cdot 36 \frac{w}{n}\right)^n = \sigma_m (0.64 + 0.36 \frac{15}{3.5})^1$ =3MPa,factor of safety is 4.95.

TWSEBM: $[\sigma] = \sigma_m \left(0 \cdot 64 + 0 \cdot 36 \frac{w}{n}\right)^n = \sigma_m (0.64 + 0.36 \frac{10}{3.5})^1$ =3Mpa, factor of safety is 3.75.

According to the evaluation method of strength stability of strip coal pillar

$$k = \frac{[\sigma]}{p_p} = \sigma_C \sqrt{\frac{D}{0.6}}\left(0.64 + 0.36\frac{w}{n}\right) / \left[\gamma H\left(1 + \frac{w_e}{w_P}\right)\right] \quad (11)$$

namely

$$k = \frac{\sqrt{\frac{D}{0.6}}\left(0.64 + 0.36\frac{W}{h}\right)^1}{\gamma H\left(1 + \frac{w_e}{w_p}\right)}\sigma_c \quad (12)$$

CSEBM：$k = \frac{\sqrt{\frac{D}{0.6}}\left(0.64+0.36\frac{W}{h}\right)^1}{\gamma H\left(1+\frac{w_e}{w_p}\right)}\sigma_c$=$\frac{\sqrt{\frac{5}{0.6}}\left(0.64+0.36\frac{W}{h}\right)^1}{\gamma H\left(1+\frac{w_e}{w_p}\right)}\sigma_c$=1.39

TRSEBM: $k = \frac{\sqrt{\frac{D}{0.6}}\left(0.64+0.36\frac{W}{h}\right)^1}{\gamma H\left(1+\frac{w_e}{w_p}\right)}\sigma_c$=$\frac{\sqrt{\frac{15}{0.6}}\left(0.64+0.36\frac{W}{h}\right)^1}{\gamma H\left(1+\frac{w_e}{w_p}\right)}\sigma_c$=4.55

TWSEBM：$k = \frac{\sqrt{\frac{D}{0.6}}\left(0.64+0.36\frac{W}{h}\right)^1}{\gamma H\left(1+\frac{w_e}{w_p}\right)}\sigma_c$=$\frac{\sqrt{\frac{10}{0.6}}\left(0.64+0.36\frac{W}{h}\right)^1}{\gamma H\left(1+\frac{w_e}{w_p}\right)}\sigma_c$=2.84

According to the Bieniawski formula, the calculation shows that the strength of the backfilling column of the three schemes is greater than 3 MPa, which can meet the long-term stability requirements of the backfilling body.

5. Surface subsidence

5.1 Calculation of surface subsidence by probability integral method

Probability integral method : The probability integral method believes that the surface movement caused by mining is a random event, and from a statistical point of view, it is considered that the entire mining can be decomposed into many or infinitely many small units under any mining conditions. The impact of the entire mining on the surface is equal to the sum of the effects of all unit mining. Therefore, the equation of the subsidence basin can be studied from the unit mining. Experiments show that the curve of the section of the sinking basin is normally distributed under ideal conditions, and is consistent with the distribution of probability density (Zhao *et al*. 2018). Therefore, the profile equation of the subsidence basin caused by the whole mining can be expressed as the integral formula of the probability density function.

1. Main calculation formulas of surface movement and deformation value

$$w_{(x)} = \frac{w_{cm}}{\sqrt{\pi}}\int_{-\sqrt{\pi}\frac{x}{r}}^{\infty} e^{-\lambda}\, d\lambda \quad (13)$$

$$i(x) = \frac{w_{cm}}{\gamma} e^{-\pi\left(\frac{x}{r}\right)^2} \quad (14)$$

$$k(x) = \frac{2\pi}{r^2} w_{cm}\left(\frac{x}{r}\right) e^{-\pi\left(\frac{x}{r}\right)^2} \quad (15)$$

$$U_{(x)} = \frac{b}{r} w_{cm}\left(\frac{x}{r}\right) e^{-\pi\left(\frac{x}{r}\right)} \quad (16)$$

$$\varepsilon(x) = -2\pi\frac{w_{Cm}}{r^2}\left(\frac{x}{r}\right) e^{-\pi\left(\frac{x}{r}\right)^2} \quad (17)$$

$$\lambda = (h - s) \quad (18)$$

$$w_{cm} = q_{m\cos\alpha} \quad (19)$$

$$\gamma = \frac{h}{tan\,\theta} \quad (20)$$

In these equations, *W(x)* is the subsidence term, mm; i(x)the incline term, mm/m; *K(x)* the curvature term, 10−3/m; *U(x)* the horizontal distortion term, mm/s; *ε(x)* the horizontal deformation term, mm/m; x the coordinate of the calculation point, m; h the mining depth, m; S the mining width, m; e a mathematical constant; r the main influencing radius, m; and b is the horizontal movement coefficient, a constant under certain mining and geological conditions; Wcm the maximum subsidence term, mm; q the subsidence coefficient; m the thickness of the coal seam, mm; α the dip of the coal seam; and tan θ the main effect tangent. The origin of the coordinates is the projection of the calculated boundary on the surface (taking the inflection point deviation into consideration).

5.2 Comparison of surface subsidence of three backfilling methods

1) Predicted parameters

When using the probability integral method to calculate the surface subsidence, it is very important to select the appropriate calculation parameters. Based on the geological characteristics of a mine in Shanxi Province, the main strata movement parameters are obtained by combining the field strata movement data with the formula 22-25, as shown in Table 3.

$$q = \frac{W_{cm}}{m} \quad (21)$$

$$\tan\,\beta = \frac{H}{r} \quad (22)$$

$$b = \frac{U_{cm}}{W_{cm}} \quad (23)$$

$$\theta_0 = \arctan\left(\frac{W_{cm}}{U_{cm}}\right) \quad (24)$$

W_{cm} is the maximum settlement measured value; m the coal seam mining thickness; H the mining depth; r the main influence radius; U_{cm} the maximum horizontal movement measured value;

The surface subsidence, horizontal movement, horizontal deformation and curvature values obtained by the three column filling methods are shown in Table 3. Fig. 11 shows the four parameters predicted by the TWSEBM. The maximum settlement value of the surface after the backfilling of the CSEBM reaches 520 mm, and the settlement value is the largest. The maximum settlement value of the surface in the central area of the working face after the backfilling of the TRSEBM is 300 mm, and the surface settlement value in other areas decreases from the center to both sides. The maximum settlement value of the surface after the backfilling of TWSEBM is 270 mm at the coordinate axis of 1000 m, and the

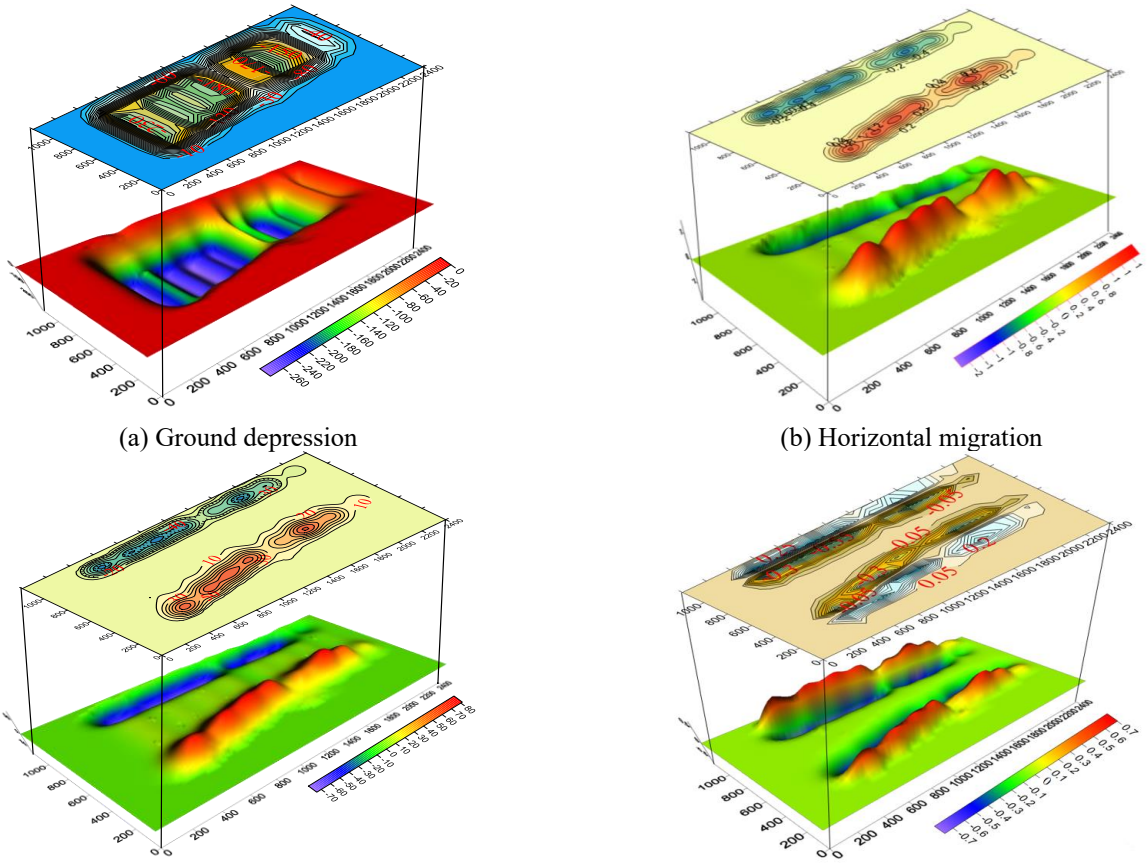

(a) Ground depression (b) Horizontal migration

(c) Lateral deformation (d) Curvature

Fig.11 The surface deformation prediction map of TWSEBM method

Table 3 Prediction parameters of surface movement

mining depth	sinking coefficient q	Horizontal shift Dynamic coefficient b	The main influence angle tangent tgβ	Inflection point offset Coefficient S/ H	Propagation influence Angular coefficient K
360	0.3	0.28	2.5	0.10	0.6
360	0.15	0.28	2.0	0.10	0.6
360	0.15	0.28	2.0	0.10	0.6

Table 4 Surface subsidence, horizontal movement, horizontal deformation and curvature values obtained by three column backfilling methods

backfilling method	Coal seam thickness / m	Maximum sinking value / mm	Maximum horizontal movement Value / mm	Maximum orizontal deformation value / mm m-1	Maximum urvature / mm m-1
			trend	trend	trend
CSEBM	3.5	520	140	-1.4	0.3
TRSEBM	3.5	300	90	0.8	0.018
TWSEBM	3.5	270	80	0.7	0.016

value on both sides is the smallest.

It can be seen from Table 4 that the maximum horizontal movement of the surface after the backfilling of the CSEBM is 140 mm, the horizontal movement of the surface after the backfilling of the TRSEBM is 90 mm, and the minimum horizontal movement of the surface after the backfilling of the TWSEBM is 80 mm. The horizontal deformation and curvature map effect of the TWSEBM is also better than that of the CSEBM and TRSEBM.

Therefore, the TWSEBM have the minimum surface subsidence, surface horizontal movement, horizontal deformation and curvature. The stability of the underground

space is strong, which meets the safety requirements. At the same time, the backfilling method of the TWSEBM improves the effective volume of the single available space in the goaf, which lays a foundation for the next research on the utilization methods of pumped storage power generation and carbon dioxide storage in the goaf.

6. Conclusions

- Based on the short-wall continuous mining and continuous backfilling process and paste backfilling mining method, three key pillar backfilling methods are proposed, which are CSEBM, TRSEBM and TWSEBM.
- Three kinds of column backfilling schemes are numerically simulated, and the vertical stress diagram after excavation is obtained. At the same time, the cost and space size of the three column backfilling schemes are analyzed. The results show that the TWSEBM scheme has lower cost and larger space.
- The probability integral method is used to calculate the surface subsidence caused by mining. Based on the geological characteristics of a mine in Shanxi Province, the surface control effects of three key pillar backfilling schemes are analyzed, and the surface subsidence, horizontal movement, horizontal deformation and curvature are obtained. The results show that the surface subsidence, horizontal movement, horizontal deformation and curvature values of the TWSEBM scheme are the smallest, followed by the TRSEBM scheme, and the value obtained by the CSEBM scheme is the largest.

Acknowledgments

This study was funded by National Natural Science Foundation of China (52104203), Shandong Province Natural Science Foundation Project (ZR2020QE128, ZR2020ME102, ZR2021ME138).

References

Bai, J.B., Zhang, Z.Z., Wang, X.Y., Xu, Y. and Yan, S. (2022), "Stress control and surrounding rock strengthening mechanism and application of high water material backfilling gob-side entry retaining", *Coal Sci. Tech.*, **50**(6), 16-28. https://doi.org/10.13199/j.cnki.cst.2022-0257.

Bai, J.W., Cui, B.Q., Qi, T.Y., Zhu, W.B., Wang, K. Shi, X.D., Wu, H.T. and Kang, L.X. (2021), "Basic theory of key pillar-side backfilling strata control", *Coal J.*, **46**(2), 424-438. https://doi.org/10.13225/j.cnki.jccs.xr20.1869.

Chang, X.K., Wang, M.G., Wang, Z.Q. and Fan, J.M. (2022), "Application of green backfilling mining technology for solid waste under villages in western ecologically fragile areas", *Coal Eng.*, **54**(7), 1-6.

Cui, B.Q., Bai, J.W., Feng, G.R., Wang, S.Y. and Wang, K. (2023), "Failure response characteristics and instability mechanism of coal-filled structure with unilateral backfilling beside the column", *J. Central South University (Natural Science Edition)*, **54**(6), 2431-2446.

Feng, G.R., Bai, J.W., Shi, X.D., Qi, T.Y., Wang, P.F., Guo, J., Wang, S.Y. and Kang, L.J. (2021), "Key pillar theory and its application prospect of chain instability of residual coal pillar group", *Coal J.*, **46**(1), 164-179. https://doi.org/10.13225/j.cnki.jccs.2020.0927.

Feng, G.R., Ma, J.B., Bai, J.W., Zhu, W.B. and Wu, H.T. (2023), "Study on the prevention and control effect of chain instability of coal pillars left by bilateral backfilling beside key pillars", *J. Min. Saf. Eng.*, **40**(5), 945-956. https://doi.org/10.13545/j.cnki.jmse.2023.0241.

Hai, G.Z. and Zhang, C.L. (1987), "Discussion on some problems of comprehensive mechanized mining in coal mining face with water sand backfilling method", *J. Liaoning Tech. Univ.*, (1), 28-34.

Hu, B.N., Liu, P.L., Cui, F. and Wang, H.Y. (2020), "Review and development status of backfilling coal mining technology in China", *Coal Sci. Tech.*, **48**(9), 9-47. https://doi.org/10.13199/j.cnki.cst.2020.09.004.

Huang, D.M., Xing, D.Q., Chang, X.K., Zhu, Y.Y. and Gao, C.J. (2021), "Analysis and application of filling mining technology in China's mining area: A case study of Yuxing coal mine", *Arch. Min. Sci.*, **66**(4), 611-624. https://doi.org/10.24425/ams.2021.139600.

Khaldoun, A., Latifa, O., BabaKhadija, B. and Lahcen, B. (2016), "Valorization of mining waste and tailings through paste backfilling solution, Imiter operation, Morocco", *Int. J. Min. Sci. Tech.*, **26**(3), 511-516.

Li, T., Chen, G.B., Qin, Z.C., Li, Q.H., Cao, B. and Liu, Y.L. (2020), "The gob-side entry retaining with the high-water filling material in Xin'an Coal Mine", *Geomech. Eng.*, **22**(6), 541-552. https://doi.org/10.12989/gae.2020.22.6.541.

Li, Y.L., Lu, B., Yang, R.S., Lin, H. and Xu, B. (2022), "Continuous mining and backfilling cemented backfilling coal mining technology and typical engineering cases", *Coal J.*, **47**(3), 1055-1071. https://doi.org/10.13225/j.cnki.jccs.2021.1612.

Liu, J.G., Li, X.W. and He, T. (2020b), "Application status and development of coal mine backfilling mining in China", *Coal J.*, **45**(1), 141-150. https://doi.org/10.13225/j.cnki.jccs.YG19.1063

Liu, J.G., Wang, H.Q. and Zhao, J.W. (2020a), "Review and Prospect of the Development of Solid Backfilling Mining Technology in Coal Mine", *Coal Sci. Tech.*, **48**(9), 27-38. https://doi.org/10.13199/j.cnki.cst.2020.09.003.

Lu, Y., Jiang, N., Wang, C.X., Zhang, M., Kong, D.Z. and Pan, H.Y. (2023), "Stability analysis of settled goaf with two-layer coal seams under building load- A case study in China", *Geomech. Eng.*, **32**(3), 245-254. https://doi.org/10.12989/gae.2023.32.3.245.

Meng, Z.X., Dong, Y., Zhang, X.G., Jiao, F.S., Fan, Y.Q. and Thammavongsa, C. (2023), "Short-wall paste continuous mining and continuous backfilling for controlling industrial square surface subsidence", *Front. Earth Sci.*, **10**. https://doi.org/10.3389/feart.2022.1009617.

Miao, X.X., Zhang, J.X. and Guo, G.L. (2010), "Research on methods and techniques of mechanized solid backfill mining", *Acta Coale Sinica*, **35**(1), 1-6. https://doi.org/10.13225/j.cnki.jccs.2010.01.006.

Rajeev, P., Sumanasekera, P.R. and Sivakugan, N. (2016), "Lateral variation of the vertical stress in underground mine stopes filled with granular backfills", *Geotech. Geol. Eng.*, **34**(2), 481-492. https://doi.org/10.1007/s10706-015-9959-4.

Shao, C.R. (2021), "Research status of paste backfilling mining in coal mines in China", *Energ. Energ. Saving*, (9), 49-51. https://doi.org/10.16643/j.cnki.14-1360/td.2021.09.018.

Sun, C.S. (2022), "Research and application of high water backfilling gob-side entry retaining technology in Malan mine",

Shandong Coal Tech., **40**(12), 58-60.
Sun, X.K. (2021), "Research on paste backfilling mining technology for ' three under ' coal mining", *Coal Sci. Tech*., **49**(1), 218-224. https://doi.org/10.13199/j.cnki.cst.2021.01.017.
Ugurlu, O.F. and Ozturk, C. (2021), "Experimental investigation for the use of tailings as paste-fill material through design of experiment", *Geomech. Eng*., **26**(5), 465-475. https://doi.org/10.12989/gae.2021.26.5.465.
Wang, C.X., Liu,Y., Hu, H., Li, Y. and Lu, Y. (2019), "Study on filling material ratio and filling effect: taking coarse fly ash and coal gangue as the main filling component", *Adv. Civil Eng*., https://doi.org/10.1155/2019/2898019
Wang, C.X., Lu, Y., Li, Y.Y., Zhang, B.C. and Liang, Y.B. (2019), "Deformation process and prediction of filling gangue: A case study in China", *Geomech. Eng*., **18**(4), 417-426. https://doi.org/10.12989/gae.2019.18.4.417.
Wang, C.X., Shen, B.T., Chen, J.T., Tong, W.X., Jiang, Z., Liu, Y. and Li, Y.Y. (2020), "Compression characteristics of filling gangue and simulation of mining with gangue backfilling: An experimental investigation", *Geomech. Eng*., **20**(6), 485-495. https://doi.org/10.12989/gae.2020.20.6.485.
Wang, F. and Zhang, D.F. (2009), "Application status and development prospect of goaf backfilling method", *Sci. Tech. Inform. Development Economy*, **19** (33), 110-111.
Wang, Y.Y., Yu, Z.Q. and Cui, L.Z. (2022), "Uniaxial compression test of paste backfilling materials with different water content", *Coal Sci. Tech*., **50**(6), 219-224. https://doi.org/10.13199/j.cnki.cst.2020-0251.
Widisinghe, S. and Sivakugan, N. (2014), "Vertical stress isobars for trenches and mine stopes containing granular backfills", *Int. J. Geomech*., **14**(2), 313-318. https://doi.org/10.1061/(ASCE)GM.1943-5622.0000321.
Wu, S.K., Zhang, J.W., Xu,Y.L., Song, Y.X. and Fan, W.B. (2023), "Study on physical and mechanical properties and engineering application of high water backfilling material in coal mine", *J. Min. Saf. Eng*., **40**(4), 754-763. https://doi.org/10.13545/j.cnki.jmse.2023.0017.
Wu, Y.Z. and Li, Y.H. (2011), "A field study on electroosmotic consolidation of hydraulic fill mud", *Proceedings of the Electric Technology and Civil Engineering (ICETCE)*, *2011 International Conference on*.
Xu, J.L., Xuan, D.Y. and Zhu, W.B. (2011), "Present situation and prospect of backfilling coal mining technology", *Min. Tech*., **11**(3), 24-30. https://doi.org/10.13828/j.cnki.ckjs.2011.03.027.
Yang, W.G. (2023), "Application of high water backfilling technology in fully mechanized working face crossing empty roadway", *Energ. Energ. Saving*, (8), 171-173+182. https://doi.org/10.16643/j.cnki.14-1360 / td.2023.08.05.
Yang, Y.D. (2023), "Study on surface subsidence and overburden movement and failure law of paste backfilling mining", *Shanxi Metallurgy*, **46**(6), 131-133. https://doi.org/10.16525/j.cnki.cn14-1167/tf.2023.06.048.
Yu, Y.H., Ma, L.Q. and Zhang, D.S. (2020), "Characteristics of roof ground subsidence while applying a continuous excavation continuous backfill method in longwall mining", *Energies*, **13**(1). https://doi.org/10.3390/en13010095.
Zhang, F., Liu, J., Ni, H., Li, W. and Liu, Y. (2021), "Development of coal mine backfilling paste with certain early strength and its flow characteristics", Geofluids, 1-14.
Zhao, J.H., Jiang, N., Yin, LM. and Bai, L.Y. (2018), "The effects of mining subsidence and drainage improvements on a waterlogged area", *Bull. Eng. Geol. Environ*., **78**, 3815-3831. https://doi.org/10.1007/s10064-018-1356-9.